Persistence of superconducting condensate far above the critical temperature in $YBa_2(Cu,Zn)_3O_y$ revealed by *c*-axis optical conductivity measurements for several Zn concentrations and carrier doping levels

Ece Uykur, Kiyohisa Tanaka, Takahiko Masui, Shigeki Miyasaka, and Setsuko Tajima

Department of Physics, Graduate School of Science,

Osaka University, 560-0043, Osaka, JAPAN

arXiv:1403.4092v1 [cond-mat.supr-con] 17 Mar 2014

Abstract

The superconductivity precursor phenomena in high temperature cuprate superconductors was studied by direct measurements of superconducting condensate with the use of the *c*-axis optical conductivity of $YBa_2(Cu_{1-x}Zn_x)_3O_y$ for several doping levels (p) as well as for several Zn-concentrations. Both of the real and imaginary part of the optical conductivity clearly showed that the superconducting carriers persist up to the high temperatures T_p that is higher than the critical temperature T_c but lower than the pseudogap temperature T^*. T_p increases with reducing doping level like T^*, but decreases with Zn-substitution unlike T^*.

Precursor superconductivity is one of the subjects that currently attract a lot of attention in the research of high temperature superconducting cuprates [1–6]. Despite the number of reports presented so far, this problem is still controversial. One common observation is that the superconducting fluctuation regime can be described in a temperature range between T_c (superconducting critical temperature) and T^* (pseudogap temperature). However, the carrier-doping dependence and the temperature range show significant differences among the different probes. Some experiments like Nernst effect [1], diamagnetism measurements [2] reported the superconducting fluctuation regime at the temperatures as high as 3-4 T_c with a doping dependence different from that of T_c. On the other hand, the microwave experiments [5] showed that the temperature range of the superconducting fluctuation is only 10-20 K above T_c with a doping dependence similar to the T_c dome.

Here we report the observation of superconducting condensate above T_c through the c-axis optical spectra of Zn-doped $YBa_2Cu_3O_y$ (YBCO) single crystals for several doping levels (p) in a wide energy range (2.5 meV – 40 eV). Doping level p in YBCO varies with the oxygen concentration [7] and the maximum T_c is achieved at $p = 0.16$ (optimum doping). In the c-axis optical conductivity, we can clearly distinguish the pseudogap and the superconducting gap, while in many probes it is difficult to distinguish these two gaps. YBCO has high conductivity along the c-axis, compared to many other cuprates, which allows us to detect small changes of conductivity. Zn-substitution, on the other hand, is useful to resolve the superconductivity related responses. Temperature dependent reflectivity measurements are performed on $YBa_2(Cu_{1-x}Zn_x)_3O_y$ single crystals, where the details regarding the samples are described in the supplementary information.

The c-axis optical conductivity is suppressed at low energies both by the pseudogap and the superconducting gap, while the direction of the spectral weight (SW) transfer is opposite in these two gaps. The lost SW is transferred to the high energy region for the pseudogap, while it is redistributed at δ-function at zero frequency for the superconducting gap. We determined the pseudogap opening temperature T^* by tracing the suppression of the low energy optical conductivity (at 20 cm^{-1}), as shown in Fig. 1. When the temperature decreases from room temperature, the low energy optical conductivity gradually increases due to the metallic response of the system, and below T^*, it begins to decrease. The metallic behavior is weakened and the turning point - T^* - increases with underdoping. The pseudogap issue has been discussed in many experiments [8]. Our T^* values for the Zn-free

samples are in good agreement with those by the other methods such as the measurements of the ^{89}Y nuclear magnetic resonance (NMR) Knight shift [9] and resistivity [10]. Moreover, as it has been pointed out by many research groups [11–14], the pseudogap temperature does not change significantly with Zn-substitution (see Fig. 1b and 1c).

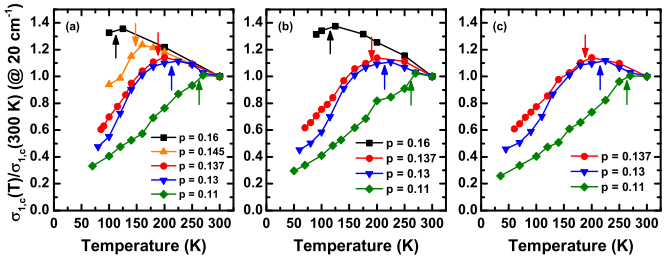


FIG. 1. T-dependence of low energy optical conductivity for various p with Zn-content $x = 0$ (a), $x = 0.007$ (b), and $x = 0.012$ (c). The arrows indicate the pseudogap temperature, T^*. All the values are normalized to the room temperature value.

Optical probe is also very sensitive to the superconducting carrier response. The imaginary part of the optical conductivity ($\sigma_2(\omega)$) is directly related to the superfluid density ($4\pi\omega\sigma_2(\omega) = \omega_{ps}^2 = 4\pi n_s/m^*$). Another way to calculate the superfluid density from optical spectra is to estimate the missing area in the real part of the optical conductivity ($\sigma_1(\omega)$). Since we found that the spectral weight of $\sigma_1(\omega)$ is conserved below 5000 cm^{-1} in our previous study [14], the missing area was estimated from the deviation from this conserved value for each sample. In Fig. 2, we plot the temperature dependence of ω_{ps}^2 determined from the missing area in $\sigma_1(\omega)$ (red circles) and from $\sigma_2(\omega)$ (black squares) for various doping levels and Zn-contents. Details of the data analysis can be found in the supplementary information. The results by both methods are qualitatively the same: zero values at high temperatures, followed by a rapid increase at T_c due to the superconducting transition. A closer look at each figure (the insets) revealed a finite value of the superfluid densities (ω_{ps}^2) at a certain temperature higher than T_c. We name this temperature the precursor superconductivity temperature T_p. For the underdoped Zn-free sample ($p = 0.11$), this value is as high as 160 K. With decreasing temperature, ω_{ps}^2 gradually increases and the slope of increase suddenly becomes steeper at the temperature near T_c. Hereafter, we refer to this temperature as T_c'. From all the figures, we can find that the superconducting carriers persist up to much higher temperatures than T_c, although its fraction is very small (less than a few % of the total ω_{ps}^2

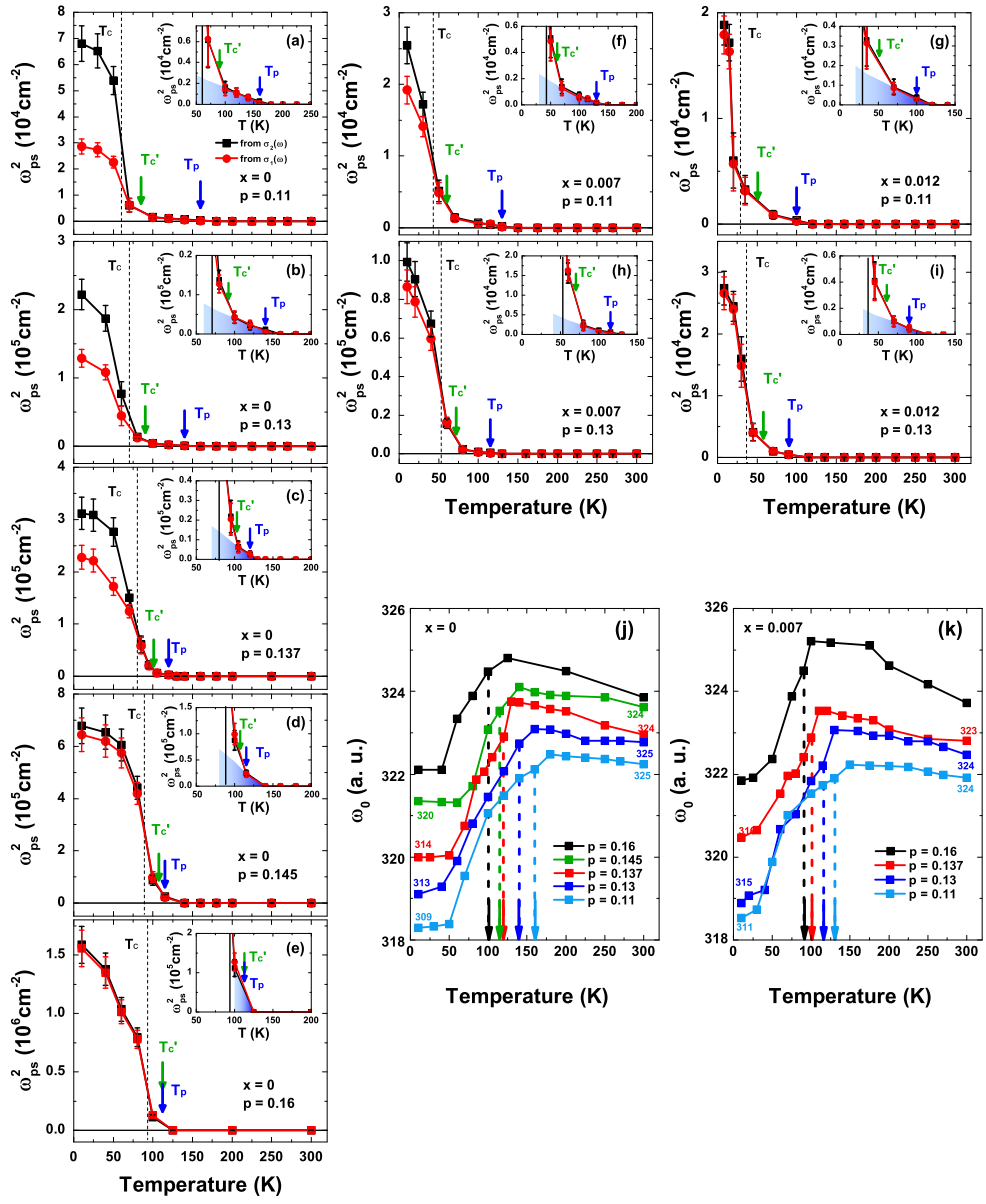


FIG. 2. Determination of the precursor superconducting state. (a) - (g) are the temperature dependences of ω_{ps}^2 obtained from the missing area in $\sigma_1(\omega)$ (red cicles) and from $\sigma_2(\omega)$ (black squares). Insets are the expanded figures near T_p. Figures (a) to (e) demonstrate the doping dependent behavior for $x = 0$, while in Figs. (a, f, g) and Figs. (b, h, i) we can see the x-dependence at $p = 0$. 11 and 0.13, respectively. (j) and (k) The resonance frequencies of the oxygen bending mode for $x = 0$ and 0.007, respectively. Error bars in these figures are discussed in the supplementary information.

at $T = 0$).

It is interesting that the doping dependences of T_c' and T_p are different (Figs. 2(a-e)). T_c' is always 10-20 K above T_c and thus follow the T_c change, whereas T_p increases with decreasing doping levels (p) and reaches much higher temperatures than T_c'. T_c' and T_p are almost merged at the optimum doping $p = 0.16$ (Fig. 2(e)). Although these two temperature scales (T_p and T_c') show different doping dependences, the Zn-dependences are similar (Figs. 2(a), 2(f), 2(g) for $p = 0.11$ and Figs. 2(b), 2(h), 2(i) for $p = 0.13$). Namely, as Zn content increases, both T_p and T_c' decrease just like T_c [15].

The transverse Josephson plasma (TJP) resonance mode [16] might be used as a measure of superconductivity, as well. A broad conductivity peak starts to appear weakly above T_c in the far-infrared region, and significantly grows below T_c. Meanwhile, it strongly couples with the oxygen bending mode phonon at ~ 320 cm^{-1}, which results in the change in the SW and the resonance frequency of this phonon mode. Therefore, by tracing the phonon frequency (ω_0) of the oxygen bending mode, we can identify the temperature at which the TJP mode starts to evolve. Dubroka *et al.* attributed the appearance of the TJP resonance mode above T_c to the precursor superconductivity effect [6]. We also plot ω_0 to estimate the onset temperature of precursor superconductivity, assuming that the TJP mode is an indication of superconductivity. From the temperature dependence of ω_0 (Figs. 2(j) and 2(k)), we can estimate the values of T_p at which ω_0 starts to decrease. In both the pure ($x = 0$) and the Zn-doped ($x = 0.007$) samples, for all the doping levels, T_p values obtained from the TJP resonance mode coincide with those estimated from $\sigma_2(\omega)$ and $\sigma_1(\omega)$. The fact that the three independent methods give the same T_p values confirms that our observation of superconductivity up to T_p is real.

We plot all the temperatures T^*, T_p, T_c' , and T_c for various doping levels and Zn-contents in Fig. 3(a), where for each Zn-content (x) T_c is normalized by the value at $p = 0.16$ (namely, the normalized T_c equals to 1 at $p = 0.16$) and T_c', T_p, and T^* are multiplied by the same normalization factor for each x. It turns out that T_c' and T_p for different x samples form a single curve, which indicates that both of these temperatures change with x, scaling with T_c, unlike the pseudogap temperatures (T^* does not change with x). The Zn-dependence of T_p and T_c' gives further evidence that we really observe the superconducting signature above T_c. It is natural to consider that T_c' corresponds to a conventional superconducting fluctuation temperature described by the Ginzburg-Landau formalism [17], but T_p indicates

the unusual phenomenon due to superconductivity precursor. These systematic Zn- and doping-dependent behaviors prove that our observation of precursor superconductivity is neither due to the sample inhomogeneity nor due to the measurement errors.

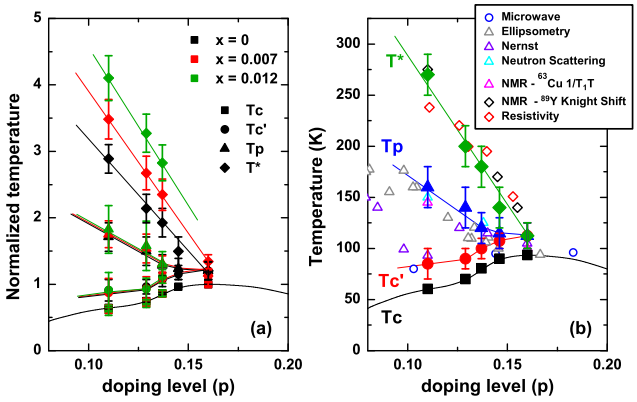


FIG. 3. Electronic phase diagram of $YBa_2(Cu_{1-x}Zn_x)_3\ O_y$. (a) The normalized variable for T_c' (circles), T_p (triangles), and T^* (diamonds) for $x = 0$ (black symbols), $x = 0.007$ (red symbols), and $x = 0.012$ (green symbols). (b) Phase diagram of the $YBa_2Cu_3O_y$ where the temperatures obtained by our measurements (solid symbols) are plotted together with the data by several other probes (Microwave [5], ellipsometry [6], Nernst effect [27], neutron scattering [29], NMR ^{63}Cu $1/T_1T$ [30, 31], NMR ^{89}Y Knight shift [9], and resistivity [10].

The other new finding in the present study is that the difference of ω_{ps}^2 estimated from $\sigma_2(\omega)$ and the missing area in $\sigma_1(\omega)$ diminishes with Zn-substitution. As we see in Fig. 2, for the Zn-free samples, although the temperature dependences of ω_{ps}^2 are similar, the two estimation methods give significantly different values of ω_{ps}^2 in the underdoped regime. This discrepancy has been previously pointed out [18], and attributed to the kinetic energy reduction [19]. In this scenario, not only the low energy SW but also the high energy SW in the visible region are condensed into a delta function at $\omega = 0$.

A similar reduction of the discrepancy in ω_{ps}^2 has been reported in the optical measurements under magnetic fields for YBCO [20]. The common effect of magnetic field and Zn-substitution is that the TJP resonance mode is suppressed in both cases. The TJP mode can be seen as a broad peak in $\sigma_1(\omega)$ below T_c, which reduces the calculated missing area [16, 21]. On the other hand, the low energy $\sigma_2(\omega)$ is not affected by this mode. Therefore, we conclude that the observed difference in ω_{ps}^2 in the two methods is caused by the inappropriate estimation of the missing area, i.e. ignoring the contribution of the TJP mode to ω_{ps}^2.

In other words, when the TJP mode is suppressed, the difference in ω_{ps}^2 should vanish. Note that the TJP mode above T_c is very weak [22] and thus it does not couse an appreciable difference in ω_{ps}^2 in Fig. 2.

In Fig. 3(b) we compare our results for the Zn-free sample with the published data of YBCO determined by the other probes. Solid symbols represent our data. Our T_c' values are in good agreement with the recent results of microwave measurements on YBCO [5]. Moreover, the temperature scale of T_c' relative to T_c is also consistent with the results of THz [4, 23, 24] and microwave measurements [25] for the other cuprate systems, $La_{2-x}Sr_xCuO_4$ and $Bi_2Sr_2CaCu_2O_{8+\delta}$. On the other hand, neither THz nor microwave measurements detected the temperature scale T_p. This might be due to the ambiguity in determining the normal carrier component which we need to subtract in the analysis to calculate ω_{ps}^2 from $\sigma_2(\omega)$ [26].

Our T_p values are in good agreement with the temperatures observed by ellipsometry [6] and partly by Nernst effect [27, 28]. In Ref. 6, T_p was estimated only from the phonon softening related to the TJP resonance, which is not direct evidence for superconducting condensate. Moreover, we cannot adopt this method to follow the T_p change with Zn-substitution, since the TJP mode is gradually suppressed with Zn-substitution. It is worth noting that T_p well coincides with the spin gap temperature reported by neutron scattering [29] and the relaxation rate T_1^{-1} of NMR [30, 31].

Our results indicates that a precursor of superconductivity does exist at temperatures much higher than T_c but lower than T^*. This precursor phenomenon is clearly distinguished from the pseudogap not only because of the difference in temperature scale but also because of the fact that the electrons removed from the Fermi surface owing to the pseudogap never contribute to superconductivity [14, 32]. Moreover, the observation of superconducting condensate implies that the Cooper pairs are formed with phase coherence at T_p.

These experimental facts put a strong constraint on the theory for high-T_c superconductivity. For example, preformed pairs predicted by the mean field theory of t-J model [33] do not have phase coherence and thus they cannot explain our observation. Microscopically phase separated state in a doped Mott insulator [34–36] is a more plausible candidate. Recently the charge density wave (CDW) order was observed in the underdoped YBCO at the temperature close to our T_p [37, 38]. The simultaneous observation of a precursor of superconductivity and the CDW order suggests microscopic phase separation. Moreover,

we may expect some interplay between these two orders although they originally compete with each other. To discuss the origin of this unusual precursor, the increase of T_p with decreasing the doping level is a smoking gun pointing to the importance of Mottness in the high-T_c superconductivity mechanism.

We thank T. Tohyama and D. Van der Marel for the useful discussion. This work was supported by the Grant-in-Aid for Scientific Research from the Ministry of Education, Culture, Sports, Science and Technology of Japan (KIBAN(A) No.19204038 and KIBAN(B) No. 24340083).

[1] Y. Wang, L. Li, and N. P. Ong, Phys. Rev. B **73**, 024510 (2006)

[2] L. Li *et al.*, Phys. Rev. B **81**, 054510 (2010)

[3] T. Kondo *et al.*, Nature Physics **7**, 21 (2011)

[4] L. S. Bilbro *et al.*, Nature Physics **7**, 298 (2011)

[5] M. S. Grbić *et al.*, Phys. Rev. B **83**, 144508 (2011)

[6] A. Dubroka *et al.*, Phys. Rev. Lett. **106**, 047006 (2011)

[7] R. Liang, D. A. Bonn, and W. N. Hardy, Phys. Rev. B **73**, 180505(R) (2006)

[8] T. Timusk and B. Statt, Rep. Prog. Phys. **62**, 61 (1999)

[9] H. Alloul, J. Supercond. Nov. Mag. **25**, 585 (2012)

[10] R. Daou *et al.*, Nature **463**, 519 (2010)

[11] H. Alloul, P. Mendels, H. Casalta, J. F. Marucco, and J. Arabski, Phys. Rev. Lett. **67**, 3140 (1991)

[12] K. Mizuhashi, K. Takenaka, Y. Fukuzumi, and S. Uchida, Phys. Rev. B **52**, 3884 (1995)

[13] A. Yamamoto *et al.*, Phys. Rev. B **65**, 104505 (2002)

[14] E. Uykur, K. Tanaka, T. Masui, S. Miyasaka, and S. Tajima, J. Phys. Soc. Jpn. **82**, 033701 (2013)

[15] For example, Y. Maeno *et al.*, Nature **328**, 512 (1987)

[16] D. van der Marel and A. Tsvetkov, Czech. J. Phys. **46**, 3165 (1996)

[17] A. Larkin and A. Varlamov, *Theory of fluctuations in superconductors*, 2009 (Oxford University, 2009)

[18] D. N. Basov *et al.*, Phys. Rev. B **63**, 134514 (2001)

[19] J. Hirsch, Physica C **199**, 305 (1992)

[20] A. D. LaForge *et al.*, Phys. Rev. B **79**, 104516 (2009)

[21] D. Munzar, T. Holden, and C. Bernhard, Phys. Rev. B **67**, 020501(R) (2003)

[22] C. Bernhard, D. Munzar, A. Golnik, C. T. Lin, A. Wittlin, J. Humlíček, and M. Cardona, Phys. Rev. B **61**, 618 (2000)

[23] D. Nakamura, Y. Imai, A. Maeda, and I. Tsukada, J. Phys. Soc. Jpn. **81**, 044709 (2012)

[24] J. Corson, R. Mallozzi, J. Orenstein, J. N. Eckstein and I. Bozovic, Nature **398**, 221 (1999)

[25] T. Ohashi, H. Kitano, I. Tsukada, and A. Maeda, Phys. Rev. B **79**, 184507 (2009)

[26] S. V. Dordevic *et al.*, Phys. Rev. B **65**, 134511 (2002)

[27] N. P. Ong, Y. Wang, S. Ono, Y. Ando, and S. Uchida, Annalen der Physik (Leipzig) **19**, 9 (2003)

[28] We measured the optical spectra of the more underdoped ($\sim p = 0.06$) to extend our results to a wider doping range. The T_p for our sample at $p = 0.06$ was estimated at about 160 K from the TJP mode. Since the superfluid analysis was not accurate enough to estimate T_p, we did not plot this data in Fig. 3. Our T_p at $p = 0.06$ is consistent with the results of Nernst effect [27] and the ellipsometry [6].

[29] P. Dai *et al.*, Science **284**, 1344 (1999)

[30] M. Takigawa *et al.*, Phys. Rev. B **43**, 247 (1991)

[31] G. q. Zheng *et al.*, Physica C **263**, 367 (1996)

[32] L. Yu *et al.*, Phys. Rev. Lett. **100**, 177004 (2008)

[33] P. A. Lee, N. Nagaosa, and X.-G. Wen, Rev. Mod. Phys. **78**, 17 (2006)

[34] V. J. Emery and S. A. Kivelson, Nature **374**, 434 (1995)

[35] V. Z. Kresin, Y. N. Ovchinnikov, and S. A. Wolf, Physics Reports **431**, 231 (2006)

[36] V. J. Emery, S. A. Kivelson, and O. Zachar, Phys. Rev. B **56**, 6120 (1997)

[37] G. Ghiringhelli *et al.*, Science **337**, 821 (2012)

[38] J. Chang *et al.*, Nature Physics **8**, 871 (2012)

SUPPLEMENTARY

I. Samples

The high quality $YBa_2(Cu_{1-x}Zn_x)_3O_{7-\delta}$ single crystals with several Zn-contents (x) were grown by the pulling technique [1]. The doping level (p) was varied by adjusting the oxygen concentrations and determined from the experimental p - T_c curve [2]. The Zn-free and the Zn-substituted samples were simultaneously annealed at a specific temperature for a specific doping level under oxygen flow, then rapidly quenched into liquid nitrogen. The superconducting transition temperatures (T_c) were determined from the dc susceptibility measurements. The susceptibility curves for all the samples are given in Fig. S1 (a)-(c) for $x = 0$, 0.007, and 0.012, respectively. All the samples show rather sharp, single phase transitions. The annealing conditions, doping levels and T_c values with transition width ΔT_c are summarized in Table I.

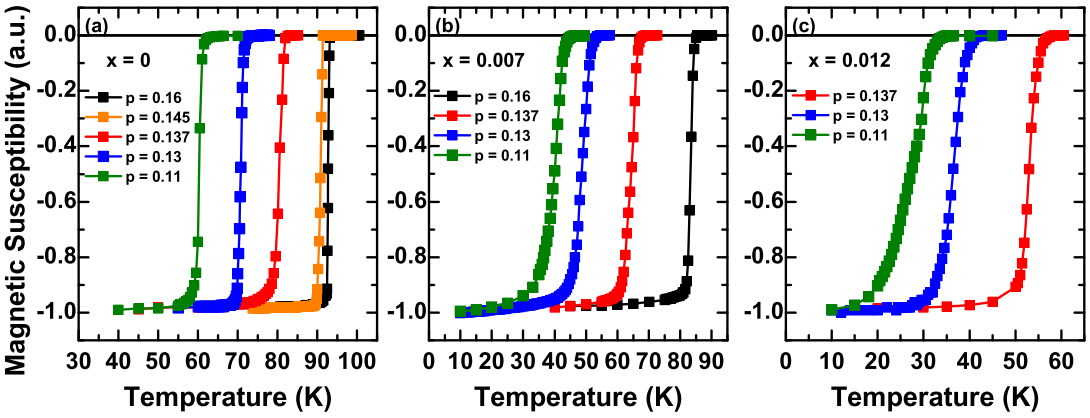


FIG. 4. Magnetic susceptibility vs temperature curves of the (a) $x = 0$, (b) $x = 0.007$, and (c) $x = 0.012$ for several doping levels (p). Magnetizations are normalized at the lowest temperature ($T = 10$ K).

TABLE I. Zn-content (x), doping level (p), T_c, transition width ΔT_c and annealing condition

Zn-content (x)	**Doping level (p)**	T_c (K)	ΔT_c (K)	**Annealing condition**
0	0.16	93.5	0.5	500 °C, 3 weeks
0	0.145	89	0.5	540 °C, 3 weeks
0	0.137	81	2	580 °C, 3 weeks
0	0.13	71	3	625 °C, 2 weeks
0	0.11	61	3	675 °C, 2 weeks
0.007	0.16	82	1	500 °C, 3 weeks
0.007	0.137	64	4	580 °C, 3 weeks
0.007	0.13	53	6	625 °C, 2 weeks
0.007	0.11	43	7	675 °C, 2 weeks
0.012	0.137	53	5	580 °C, 3 weeks
0.012	0.13	37	5	625 °C, 2 weeks
0.012	0.11	29	7	675 °C, 2 weeks

II. Error bars

The temperature dependent reflectivity measurements were performed with a Bruker 80v Fourier Transform Infrared spectrometer. The optical conductivity spectra were obtained from the measured reflectivity spectra by using the Kramers-Kronig transformation. In Fig. S2 we plot the reflectivity and the calculated optical conductivity spectra for the Zn-free sample at $p = 0.11$ as an example up to high energy region. The following supplementary figures are obtained from these data. In our previous work [3], we also presented some of these data with other Zn-substituted samples, as well.

The reflectivity measurements were carried out in six different energy regions. The spectra in the overlapped energy regions coincide with each other. Moreover, measurement at each temperature had been repeated several times. The repetition of the measurement at each energy region allow us to specify an error bar in this energy range. Moreover, we can also define another error bar in the coinciding energy regions for different measurement ranges, which eventually gives us the overall error in our reflectivity measurements. The error bars are calculated with the same way for each temperature separately. As a result, the

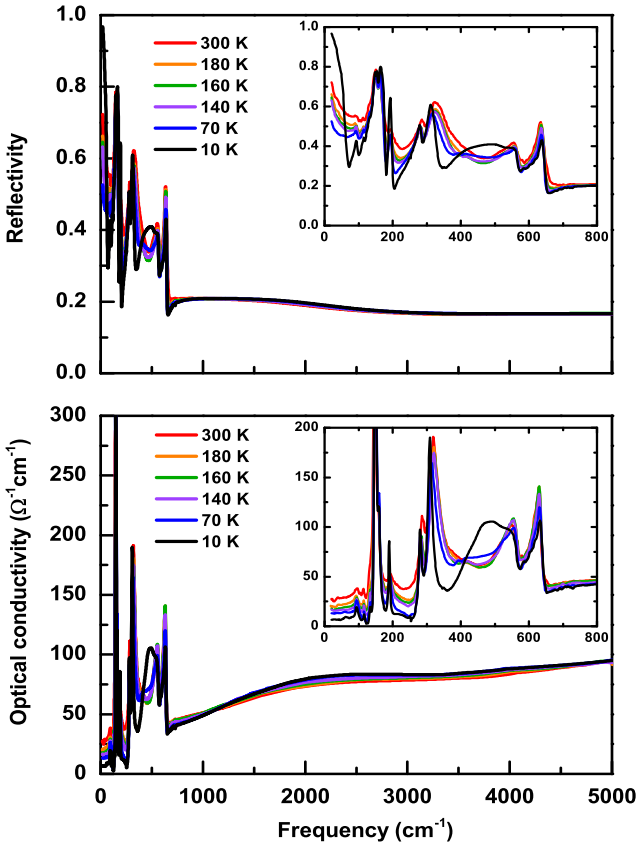


FIG. 5. Temperature dependent reflectivity and optical conductivity ($\sigma_1(\omega)$) of $YBa_2Cu_3O_y$ at $p = 0.11$. Insets show the lower energy part of each plot.

maximum error in our reflectivity measurements is better than 0.5%. The error bars in the superfluid densities were estimated from the error of the conductivity that was calculated from reflectivity. The procedure of the normal component subtraction introduces additional errors. The error bars plotted in Fig. 2 are relative ones respect to the data at T just above T^*.

III. Superfluid density estimated from the real and imaginary part of the optical conductivity

In the superconducting state, real part of the optical conductivity ($\sigma_1(\omega)$) for the superconducting carriers is condensed to a δ-function at $\omega = 0$. Then we expect to see the following relation between the imaginary optical conductivity ($\sigma_2(\omega)$) and the superfluid density ($\omega_{ps}^2 \propto n_s/m*$, n_s is the superfluid density) through Kramers-Kronig transforma-

tion; $\omega\sigma_2(\omega) \propto \omega_{ps}^2$. However, in this approach it is assumed that there is no normal carrier component in $\sigma_1(\omega)$ and $\sigma_2(\omega)$ below the gap energy, which is not the case for the high temperature cuprate superconductors. Therefore, in order to estimate the correct values of ω_{ps}^2 we have to subtract the normal carrier component from $\sigma_2(\omega)$. In this supplementary, we refer the normal carrier component as $\sigma_{2,normal}(\omega)$ that is calculated with the Kramers-Kronig transformation of $\sigma_1(\omega)$. In Figure S3, we plot our $\sigma_2(\omega)$ values, as well as the calculated normal carrier components $\sigma_{2,normal}(\omega)$ for $x = 0$ and $p = 0.11$ at several specific temperatures, 300 K, 180 K (just above T_p), 160 K (T_p), 140 K, 70 K (just above T_c), and 10 K (the lowest temperature). Similar trends have been observed for all of our samples.

We also plot the difference of $\sigma_2(\omega)$ and $\sigma_{2,normal}(\omega)$ multiplied with ω that is proportional to ω_{ps}^2, which demonstrates the ω - constant behavior of the superfluid density. If there is no superconducting carrier component, $\sigma_{2,normal}(\omega)$ should be identical to $\sigma_2(\omega)$. Indeed this behavior was observed at high temperatures (In Fig. S3, 300 K and 180 K). When we cool down the sample below 180 K, a difference between $\sigma_2(\omega)$ and $\sigma_{2,normal}(\omega)$ appears and becomes larger with decreasing temperature, which indicates a growth of the superconducting response in the system. Finally, we plot our 10 K data in a wider energy range that can be compared with the published studies [4].

For the real part of the optical conductivity, we calculated the superfluid density ω_{ps}^2 from the missing area in $\sigma_1(\omega)$. When the pseudogap opens the low energy spectral weight is suppressed, and the lost spectral weight is transferred to the high energy region. In our previous work [3], we showed that the spectral weight transfer is completed below 5000 cm^{-1}. Namely, the spectral weight is conserved below 5000 cm^{-1}. We plot the temperature dependence of the spectral weight between 50 and 5000 cm^{-1} (Fig. S4). While this spectral weight shows the temperature independent behavior down to T_p (arrow in Fig. S4), below this temperature, it starts to decrease, creating a missing area, A, that corresponds to the superconducting carrier response. We can calculate ω_{ps}^2 from this missing area by using the equation $\omega_{ps}^2 = 120/\pi A$. To compare ω_{ps}^2 with that obtained from $\sigma_2(\omega)$ we calculated the cumulative missing area with respect to the temperature just above T_p at each temperature, and plotted in Fig. 2.

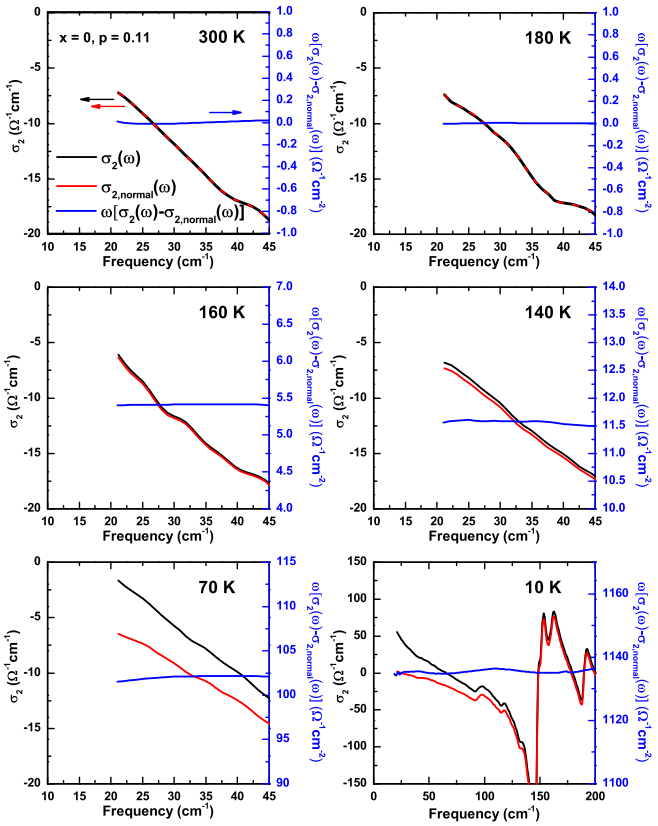


FIG. 6. $\sigma_2(\omega)$ and $\sigma_{2,normal}(\omega)$ (left axis) and $\omega\Delta\sigma_2(\omega)$ (right axis) for $x = 0$ at several temperature, where $\Delta\sigma_2(\omega) = \sigma_2(\omega)$ - $\sigma_{2,normal}(\omega)$. At high temperatures down to 180 K there is no superconducting carrier component, hence the normal carrier component is equal to $\sigma_2(\omega)$. With lowering temperature we start to see difference of the $\sigma_2(\omega)$ and $\sigma_{2,normal}(\omega)$ indicating the superconducting carrier response.

IV. Supplementary References

[1] Y. Yamada, Y. Shiohara, Physica C **217**, 182 (1993)

[2] R. Liang, D. A. Bonn, W. N.Hardy, Physical Review B **73**, 180505(R) (2006)

[3] E. Uykur et al., J. Phys. Soc. Jpn. **82**, 033701 (2013)

[4] D. N. Basov et al., Science **283**, 49 (1999)

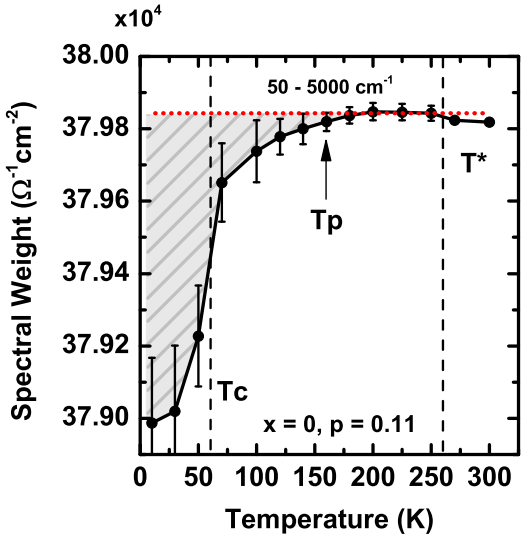


FIG. 7. Temperature dependent spectral weight (SW) calculated through the equation $SW = \int_{50}^{5000} \sigma_1(\omega) d\omega$ for $x = 0$ at $p = 0.11$. T_c and T^* values are marked with dashed lines. Hatched area represent the existence of the superconducting response. We marked the T_p with an arrow as the point that we start to see this response. Error bars are calculated as a relative error to the data just above T^*.